Nucleation and Growth of Poly(ϵ-caprolactone) on Poly(tetrafluoroethylene) by in-Situ AFM

L. G. M. Beekmans, R. Vallée, and G. J. Vancso*

Department of Materials Science and Technology of Polymers and MESA+ Research Institute, University of Twente, P.O. Box 217, 7500 AE Enschede, The Netherlands

Received February 14, 2002; Revised Manuscript Received June 11, 2002

ABSTRACT: The nucleation behavior of poly(ϵ-caprolactone) (PCL) on friction-deposited poly(tetrafluoroethylene) (PTFE) was investigated by means of atomic force microscopy (AFM). This technique allows for imaging of the nucleation and crystallization processes in real time. An estimation of the PCL crystal orientation on the PTFE substrate is made by evaluating the growth rates and the growth geometry of the lamellar crystals formed on PTFE. On the basis of the data collected, it is proposed that PCL crystallizes on PTFE predominantly via a $(100)_{PCL}$ contact plane (∼80%). The crystals adopt an orientation that minimizes the lattice mismatch at the interface between the nucleating PTFE and PCL. A $(010)_{PCL}||(100)_{PTFE}$ contact plane was simultaneously observed at a lower occurrence of approximately 20%. Visualization of the PTFE fibrillar morphology at higher resolution during isothermal crystallization revealed the appearance of a third PCL crystal orientation which developed later in time. The corresponding crystals were observed to develop from grooves on the PTFE substrate, indicating a graphoepitaxial nucleation mechanism.

Introduction

Heterogeneous nucleation is a widespread phenomenon in polymer crystallization that has been the subject of intensive study for more than 30 years.[1] Although much progress has been made in the understanding of nucleation due to the presence of a foreign second phase, the process is still not completely understood. The mechanism of epitaxial crystallization, on the other hand, has been studied in great detail. The epitaxial growth of polymers on a foreign phase is expected to involve relatively dense and low Miller index planes. Epitaxial growth relations are generally explained by a one- or two-dimensional lattice match between the contacting materials.[2] Wittmann and Lotz determined that the discrepancy between the lattice parameters should not differ more than by approximately 10−15% in order to account for true epitaxy.[2]

Graphoepitaxy is a pseudoepitaxy process induced by ridges or surface defects of the substrate, which results in a crystal orientation of the growing phase that maximizes the contact area.[3−5] Thus, crystals with large aspect ratios would be expected to align parallel to steps. In the case of polymers it is generally assumed that true epitaxy is the prevalent mode of nucleation, although it is well proven that the surface topography can also determine the orientation of the growing polymer crystals (graphoepitaxy).[3−5] Both mechanisms, true epitaxy and graphoepitaxy, have been observed for friction-deposited poly(tetrafluoroethylene) (PTFE) when used as a substrate. These thin PTFE films exhibit a single-crystal-like orientation with a fibrillar nanostructured surface topography[6,7] and are well-known for inducing oriented nucleation/growth of several polymers[3,8,9] and organic molecules.[10] Furthermore, it was demonstrated that the inductive orientation effect of PTFE on crystalline polymers is due to lattice-matching criterion,[3,8,9] topography,[3,9] or both.[3]

* To whom correspondence should be addressed: Phone (+31) 53 489 2974; Fax (+31) 53 489 3823; e-mail G.J.Vancso@ct.utwente.nl.

In this study, we report on the nucleation process of poly(ϵ-caprolactone) (PCL) on PTFE by real-time hot-stage atomic force microscopy (AFM) observations. The ability of AFM to follow real-time dynamics of polymer melting and crystallization processes is now well established.[11−15] It can be anticipated that a real-time study of PCL at lamellar resolution shall provide new insight into the nucleation process of the crystals. The work is performed in order to determine the relative occurrence of either a true epitaxy or a graphoepitaxy nucleation mechanism when this polymer is grown on PTFE. PCL was chosen for this study because of its low equilibrium melting temperature and because of its structural similarity with polyethylene (PE). It has already been reported that despite the chemical difference between PCL and PE, the structural resemblance between these polymers is sufficient to result in similar epitaxial mechanisms on a crystalline surface.[16] Substantially, it has been shown that PTFE is able to induce nucleation of PCL in the same way as it does for PE.[17] The epitaxial crystallization study of PE from the melt on friction-deposited PTFE has been studied in detail, and a lattice match between the two polymers, which is inside the expected requirements for epitaxy, has been reported as the prevalent mode of nucleation.[9] Conversely, the study of the PCL/PTFE system has not led to an understanding of the crystal orientation of the polymers, and therefore a geometrical matching criterion has not been developed.[17]

The present study is unique in reporting direct observation of the heterogeneous nucleation process of PCL lamellar crystals onto a highly ordered, friction-deposited PTFE substrate. High-resolution real-space information on individual lamellae is obtained during the nucleation process using AFM at elevated temperatures. The orientation of the PCL crystals is analyzed by observing the crystal growth geometries and by measuring the growth rates of the individual lamellar crystals along different directions. The results suggest that the main nucleation process involves the alignment

10.1021/ma020237a CCC: $22.00
Published on Web 11/02/2002

of the PCL chains with a $(100)_{PCL}$ contact plane in contact with the $(100)_{PTFE}$ substrate. In addition to this epitaxial mechanism two additional orientations of the PCL crystals were observed: the $(010)_{PCL}$ contact plane and growth initiated by substrate grooves at the surface. These additional orientation mechanisms are attributed to epitaxy and graphoepitaxy mechanisms, respectively.

Experimental Section

Poly(ϵ-caprolactone) (molar mass 55 000 g/mol) and poly(tetrafluoroethylene) (PTFE) were obtained from Aldrich. The oriented thin PTFE films were made by manually sliding the PTFE specimen over a cleaned glass substrate at 200 °C. PCL was precipitated from chloroform into methanol prior to use. The precipitate was first dried in air and then dried under vacuum for 1 day. Samples were prepared for AFM by casting from a PCL/xylene solution onto glass cover slide which has been previously rubbed with PTFE. The PCL polymer film has been estimated to be about 200 nm thick by examining the boundary of the film using AFM.

AFM experiments were performed under a nitrogen atmosphere using a NanoScope III setup (Digital Instruments). The instrument was equipped with a J-scanner (maximum scan size 100 μm^2), E-scanner (maximum scan size 10 μm^2), or A-scanner (maximum scan size 10 μm^2). Commercially available Si_3N_4 cantilevers were used with force constants of 0.38 N/m as stated by the manufacturer for contact mode measurements or Si cantilevers with a force constant of 27−83 N/m for the tapping mode experiment. Measurements were carried out in tapping mode unless otherwise reported, using the smallest possible set-point value so as to minimize interaction forces between tip and sample.[18] Height and deflection or height and phase images were acquired simultaneously either in contact mode or in tapping mode. The heating stage used for the AFM observations is described elsewhere.[15,19]

Results and Discussion

The PTFE-rubbed cover slides have been imaged using AFM, as illustrated in Figure 1, to check the quality of the substrate. The friction-transferred layer is known to consist of fibrillar domains.[6,7] The rather perfect order of the PTFE fibrils on a molecular scale is shown in Figure 1A, which is an unfiltered contact mode height image of the surface of the PTFE fibrils taken before the deposition of poly(ϵ-caprolactone) (PCL).[7] The arrows indicate the sliding direction of PTFE.

The lower-magnification image of Figure 1B reveals the microtopography of the oriented PTFE-film covered by a thin film of molten PCL. This image was obtained at a temperature of 56 °C. The surface of the supporting friction-deposited PTFE film consists of valleys and ridges that are aligned parallel to the sliding direction. It can be seen that there are often grooves along the fibril direction, which contribute to the grating-like nature of the morphology.

Height and corresponding phase images of the crystallized PCL at the boundary of the friction-deposited PTFE are shown in Figure 2. The inserted arrows indicate the chain direction of the PTFE fibrils. It is easily recognized that PCL crystallized on the glass surface results in a spherulitic morphology (indicated as area G), while PCL grown on PTFE reveals a typical oriented morphology which will be shown to be related to epitaxial growth (area T). On the boundary, a special morphology arises in which the PCL lamellar crystals grow across the boundary and extend into the area that is directly supported on the glass.[17]

A remarkable feature of the pictures shown in Figure 2 is the observation of the underlying PTFE fibrils at

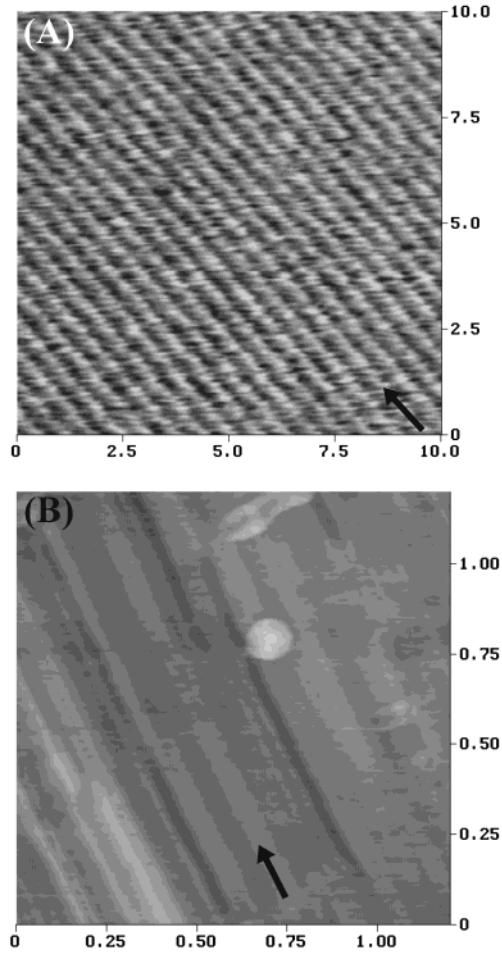

Figure 1. (A, B) AFM height images of a PTFE fibril. (A) Unfiltered high-resolution contact mode height image of the PTFE substrate showing oriented PTFE chains. The scan size is 10 × 10 nm. (B) Tapping mode AFM image obtained at a temperature of 56 °C after melting the PCL crystals deposited on PTFE at approximately 80 °C. The vertical scale is 25 nm (dark to bright), and the scan size is 1.25 × 1.25 μm. The inserted arrows indicate the stretching direction of the PTFE.

the imaged surface even after complete crystallization of the PCL. Parts A and B of Figure 3 show higher-magnification height and phase images, respectively, at the boundary of a PTFE fibril, as observed at the surface. The PTFE fibril is located at the lower right part of the images, and the added arrows again show the PTFE deposition direction, i.e., the chain direction. The PCL crystals supported by the fibril are observed at lower height and lower phase signal levels in the height and phase images, respectively. It is evident that a PTFE surface topography consisting of valleys and ridges is no longer observed since the fibril is covered by aligned edge-on seen PCL crystals. The thickness of the covering PCL layer was approximately 40 ± 10 nm, as estimated by measuring the crystal phase protruding above the PTFE fibril.[18,19] It can be seen that the PCL crystals extend into the area supported by the glass slide. Presumably, the PCL lamellar crystals have been nucleated by the PTFE fibrils and continue to grow into the melt surrounding the fibrils.

The chain axis of PCL is oriented parallel to the PTFE depositing direction ($c_{PCL} \| c_{PTFE}$). Previously mentioned studies of PE/PTFE films involved an epitaxial relationship based on a one-dimensional lattice-matching along the interchain distance of the PTFE chains.[3,9] To attain a molecular understanding of the interactions in the

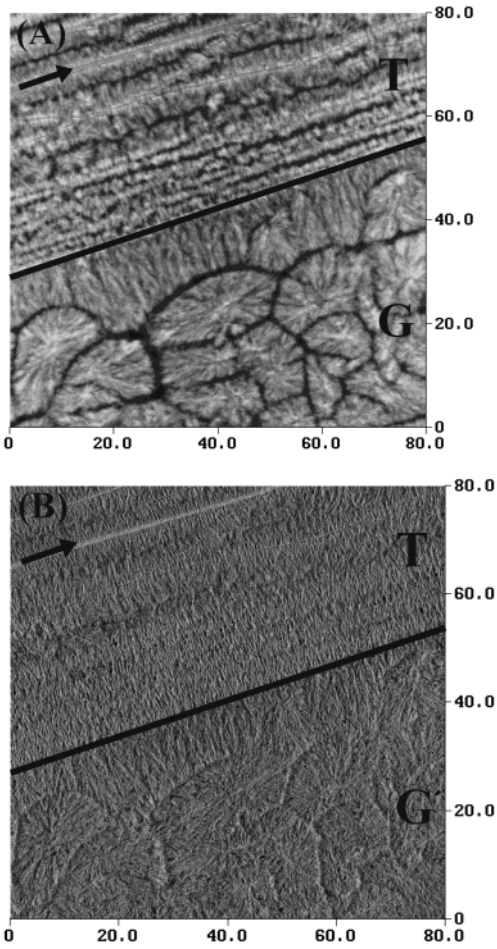

Figure 2. (A, B) Tapping mode AFM images of PCL crystallized on friction-deposited PTFE. (A) Height image, vertical scale is 300 nm (dark to bright). (B) The simultaneously recorded phase image. The added arrows indicate the orientation of the PTFE chains and the black line represents the boundary of the PTFE film. The PCL crystals in area G are supported by the glass substrate while the crystal in area T crystallized on the PTFE surface.

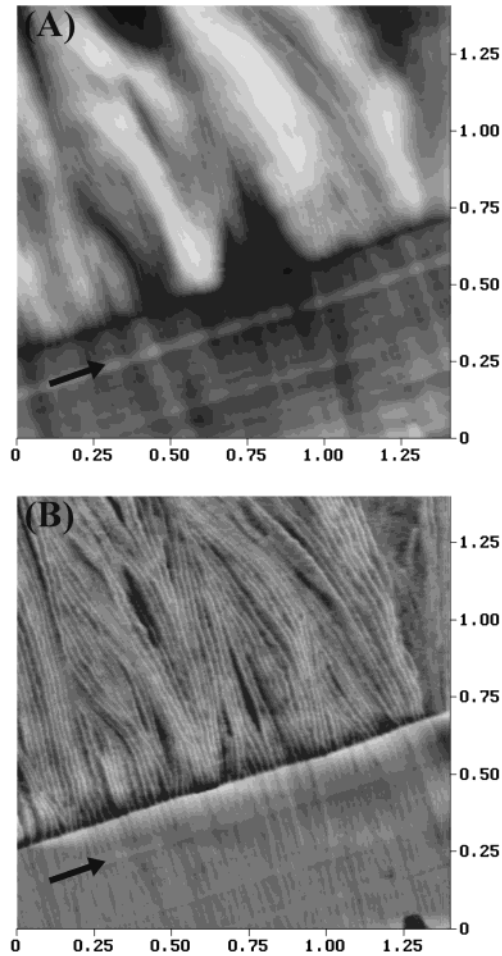

Figure 3. (A, B) Higher-magnification AFM images of PCL crystallized on the boundary of a friction-deposited PTFE fibril. (A) Height image, vertical scale is 100 nm (dark to bright). (B) The simultaneously recorded phase image. The added arrows indicate the molecular orientation of the PTFE chains.

PCL/PTFE system, the PCL plane in contact with the PTFE surface should be identified. Our approach to this analysis of the PCL crystal orientation rests on the examination of the crystal face growth rates measured by real-time AFM.

The study of PCL single crystals grown from the melt has been reported recently.[14] The crystals exhibited a truncated-lozenge shape with high axial ratios. The axial ratio is the ratio between the length along the crystallographic *b*- and *a*-axes of the crystal. High axial ratios in PCL were attributed to the fact that the growth rates of the lateral {200} growth faces were considerably smaller than the rate of growth of the {110} faces bordering the *b*-axis. In addition, it was suggested from the analysis of the kinetic data that the PCL crystallization process is not influenced by the presence of a melt/air interface. Furthermore, several studies have already demonstrated that the kinetic data obtained by AFM were consistent with the overall spherulitic growth rate as determined by light microscopy (LM).[11,13]

Since AFM is a surface technique that captures the projection of the crystal edges, there is a possibility of misinterpretation of the lamellar growth rate.[11,14] It was experienced that the orientation of the crystal with respect to the surface determines the growth rate of the crystal as measured by AFM. A distinct angle between the crystallographic axis of an edge-on-growing lamellar crystal and the *x*, *y* plane will result in an underestimation of the growth rate measured. However, in the case of epitaxial crystallization it is possible to interpret the kinetic data with more certainty since the orientation is predetermined by the nucleation of the PCL crystals on the PTFE surface.

The use of AFM to follow lamellar crystal growth of PCL nucleated on friction-deposited PTFE in real time is illustrated by the images in Figure 4. These images were obtained during an isothermal crystallization experiment at approximately 56 °C at different time intervals. The PTFE fibrils are approximately horizontal in the images and are identified by the added arrows. The images contain a total of four separated individual PTFE fibrils. The imaged area was chosen in such a way that it contained both edge-on and flat-on lamellar crystal projections. In Figure 4A the crystallographic *a*- and *b*-axes of the PCL unit cell are indicated in the flat-on crystal seen in the center of the picture. The position of this crystal relative to the PTFE fibril indicates that it is not nucleated by the PTFE; i.e., the center of the crystal aggregate is not located on the PTFE fibrils. The crystal has presumably been formed on an impurity and is used to determine the rate of advancement of the {110} and {200} growth faces unambiguously.[14]

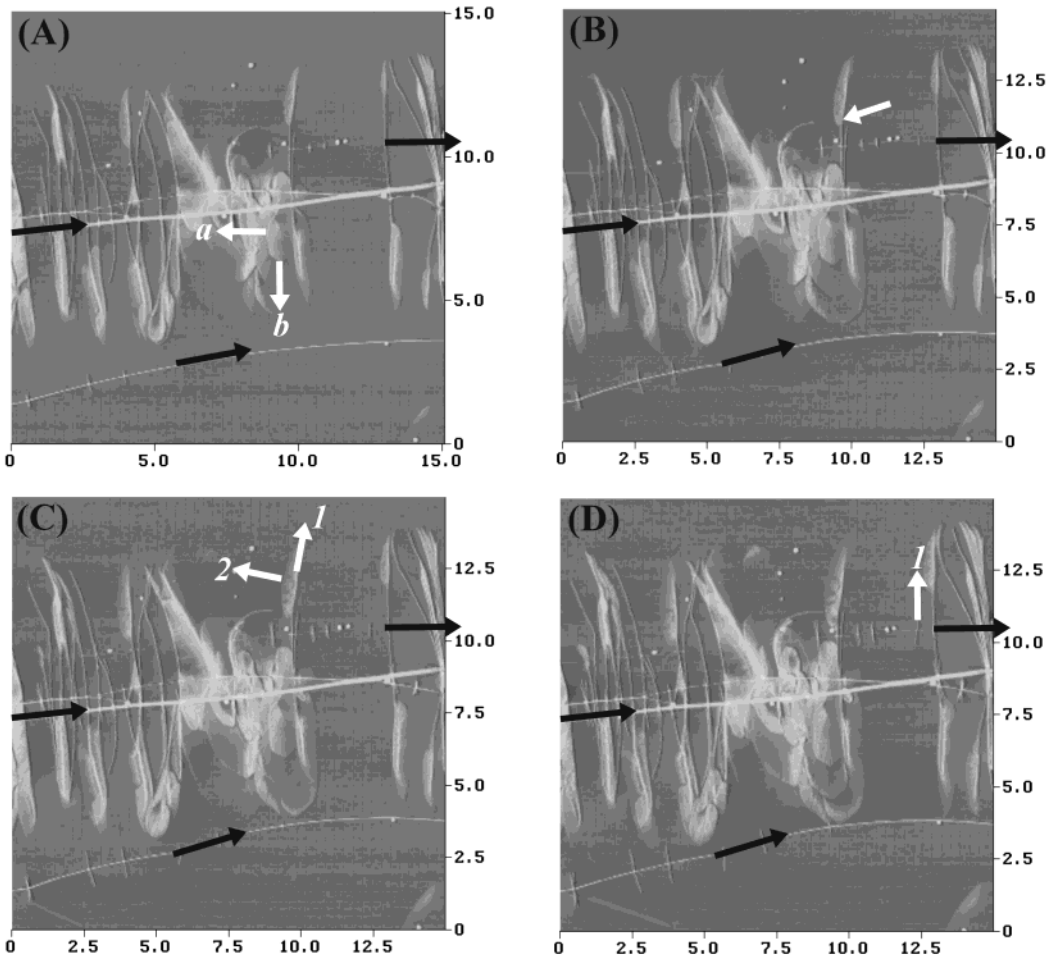

Figure 4. (A, D) AFM phase images of PCL crystals growing at a temperature of 56 °C. The successive images in (B), (C), and (D) corresponds to elapsed times of 24, 47, and 77 min, respectively, with respect to the image in (A). The added black arrows indicate the molecular orientation of the PTFE and identify individual PTFE fibrils. The added white arrows in the image of (A), (C), and (D) indicate the growth direction of the crystal growth faces while the white arrow in (B) indicates the twisting behavior of an individual lamellae.

The lamellar lengths as a function of time of the lozenge-shaped crystal pointed out in Figure 4A are shown in the graph of Figure 5A. The plot yielded an excellent linear fit with a 99% confidence interval. The lamellar crystal grows at constant rates with rate values of 7.5 and 2.8 nm/min along its crystallographic *b*- and *a*-axes, respectively. Identification of the growth faces of the epitaxial nucleated crystals seen edge-on can now be sought for by comparing the edge-on lamellar growth rates with the kinetic data obtained for the crystal seen flat-on.

An intriguing morphological observation in the series of images in Figure 4 is the continuous orientational change of the crystals, from edge-on to closer to flat-on, as indicated by the white arrow in Figure 4B. This twisting enables an identification of the growth geometry and thus allows us to determine the growth rates for the different growth faces bordering the PCL lamellar crystals nucleated by the PTFE substrate. The twisting behavior can originate from surface stresses of the crystal-fold surface originating from chain folding[20] and has previously been observed in the epitaxial crystallization of PE on PTFE.[21]

The length measurements as a function of time shown in Figure 5B correspond to the lamellar growth fronts indicated by the arrows in Figure 4C. The data yielded a constant growth rate of 7.5 nm/min for the advance of the plane parallel to the PTFE substrate (1) and 3.0 nm/min for the advance of the face perpendicular to it (2). The added dashed lines represent the linear fits obtained for the [010] and [100] directions of the crystal seen flat-on (Figure 5A). The agreement between the rates of growth of the crystals is satisfactorily indicating that the crystallographic *a*- and *b*-axes of the PCL crystals are perpendicular and parallel to the PTFE interchain distance, respectively (Figure 4C, 2 and 1). The PCL crystals grow with their fastest growth direction in the film plane.[22] The determined crystal orientation suggests the occurrence of a true epitaxy mechanism, with the following relationships at the interface:

$$c_{PCL} \| c_{PTFE}$$

$$b_{PCL} \| a_{PTFE} = b_{PTFE}$$

$$(100)_{PCL} \| (100)_{PTFE}$$

and a one-dimensional lattice mismatch (Δ) of

$$\Delta = \frac{b_{PCL} - a_{PTFE}}{a_{PTFE}} = 12\%$$

A molecular representation of the interface is shown in the image of Figure 6A with $b_{PCL} = 4.98$ Å[23] and $a_{PTFE} = b_{PTFE} = 5.66$ Å.[24] A similar lattice mismatch

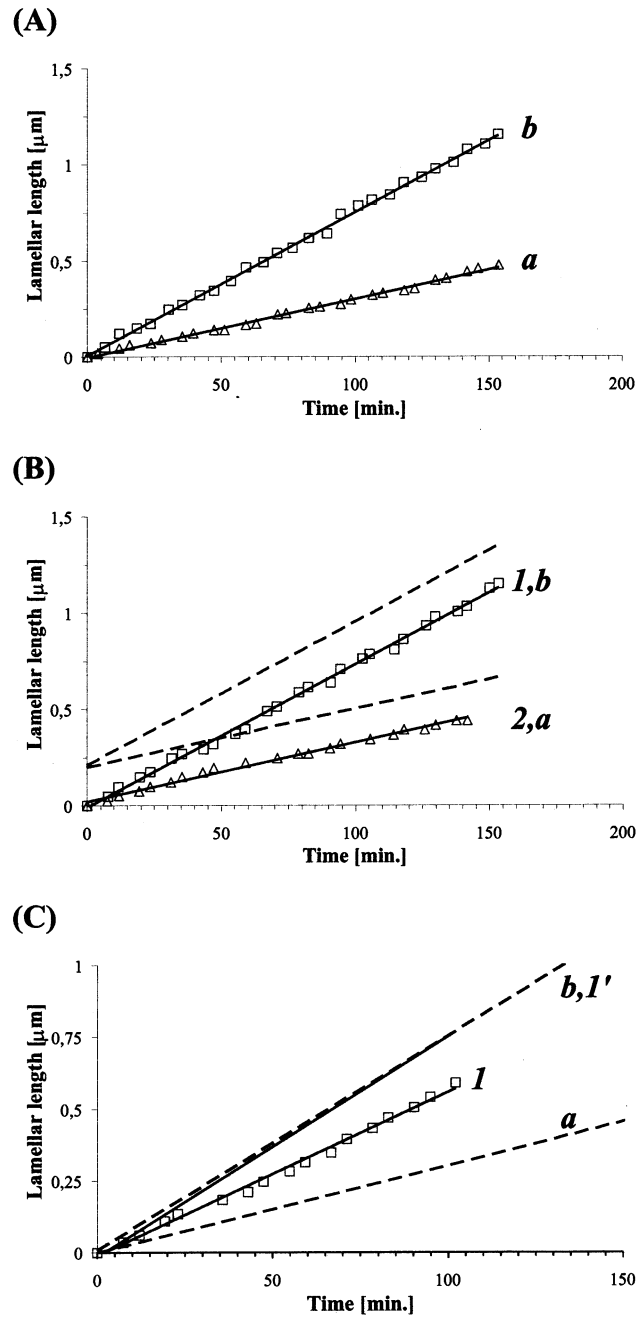

Figure 5. (A, B) Lamellar length vs time data for different PCL crystals as measured at 56 °C. (A) Data obtained along the *a* and *b* crystallographic axes for the flat-on seen reference crystal indicated by the added white arrows in the images of Figure 4A. (B) Data obtained for the different growth faces of the crystals indicated by the white arrows, 1 and 2, in the images of Figure 4C. (C) Data obtained for crystal as indicated by the white arrow, 1, in the images of Figure 4D. Line 1′ is the tilt-angle (β) corrected data. The dashed lines represent the kinetic data of the flat-on seen crystal plotted in the graph of (A).

has been reported for PE crystallized epitaxially on PTFE,[9] which is not surprising considering the structural similarities between PCL and PE.[16]

The investigation of numerous lamellar growth rate values has revealed an interesting crystal orientation-growth rate dependence. Since the PTFE topography consists of ridges and valleys (Figure 1B), the PTFE surface should also be rough on a nanometer scale; i.e., more than one crystallographic plane must be exposed at the surface. The possible nucleation sites for the

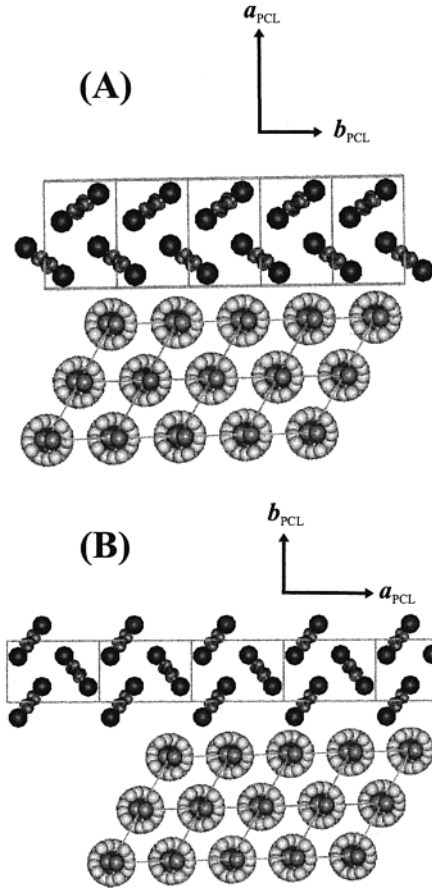

Figure 6. Molecular models of the (A) $(100)_{PCL}-(100)_{PTFE}$ interface and (B) $(010)_{PCL}-(100)_{PTFE}$ interface. The *c*-axis of both polymers is normal to the plane of the figure.

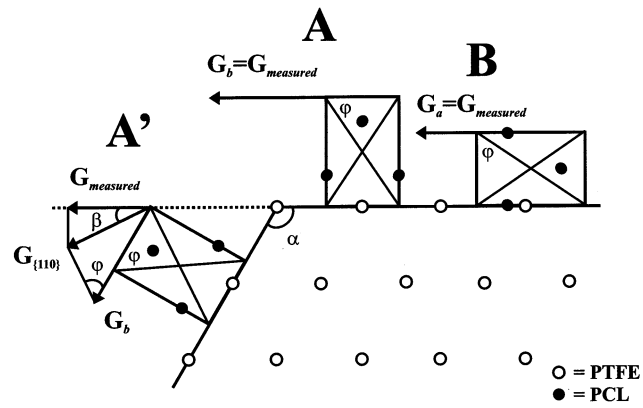

Figure 7. Schematic representation of the possible nucleation sites of PCL crystals on a PTFE substrate. The *c*-axis of both polymers is normal to the plane of the figure. In A and A′, $b_{PCL}||a_{PTFE} = b_{PTFE}$, while in B, $a_{PCL}||a_{PTFE} = b_{PTFE}$. Situations A and A′ correspond to the crystals identified in the images of parts C and D of Figure 4, respectively.

$(100)_{PCL}||(100)_{PTFE}$ interface are schematically represented in Figure 7 (situation A and A′) as previously reported by Fenwick et al. for friction-deposited PTFE substrates.[9] When the PCL crystal is nucleated onto the slope of the fibril (situation A′), its growth rate measured by AFM will be underestimated due to the fact that the actual measurements are made on the projection at a certain angle with the surface.[11,14] Figure 5C shows the plot of the lamellar length as a function of time for a crystal nucleated on such a slope, resulting in a constant rate value of 5.7 nm/min. The correspond-

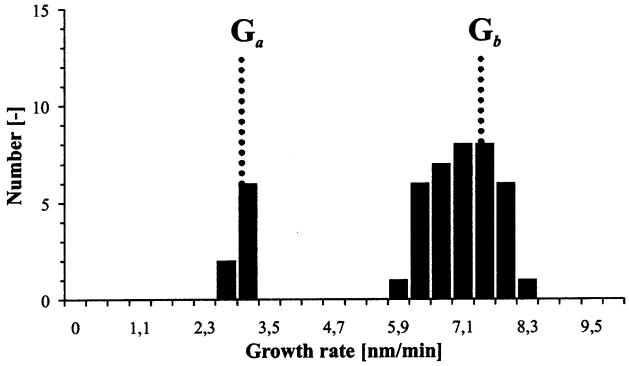

Figure 8. Lamellar crystal growth rates as measured at 56 °C for epitaxially nucleated PCL crystals. The estimated growth rates from the crystal seen flat-on are added as the dotted lines, G_b and G_a.

ing PCL crystal is identified by the added white arrow (1) in Figure 4D.

The tilt angle (β) which determines the dimensions of the observed surface projection can be calculated according to the relation $\beta = 90 - \alpha + \varphi$, in which α and φ are unit cell parameters of PCL and PTFE as defined in Figure 7, respectively. The measured growth rate can thus be corrected by the following dependence: $G_b = G_{\text{measured}}/(\cos\beta \sin\varphi)$. If this tilt-angle correction for the length measurements determined by AFM is taken into account, the thicker solid line in Figure 5C results. It can be seen that, taking into account the tilt-angle value, an excellent agreement is found with the growth-rate value obtained experimentally along the *b* axis for the reference crystal (dashed line, Figure 5C). This result strongly indicates that the crystal is nucleated on the slope of the fibril by the identified (100) epitaxial mechanism.

The growth rates for a number of epitaxially grown PCL crystals, after correction for tilted growth if necessary, are compared in the histogram shown in Figure 8. The data contain the rate values, which could be accurately measured (99% confidence interval). The dotted lines represent the growth rate as measured for the reference flat-on crystal (Figures 4A and 5A). A wide spread in the rate of advancement of the lamellae is observed for the different faces. Similar lamellar growth-rate distributions have recently been reported for the isothermal crystallization of poly(ethylene oxide)[12,13] and PE.[25] Several mechanisms have been proposed to explain this spread, including growth face poisoning and crystal rearrangement.[11] The proposed models were supported by a discontinuous growth of the lamellar crystals. The observation of constant linear growth rates (Figure 5) seems to suggest that the discontinuous growth is caused by a competition between the different lamellae growing at the spherulitic growth front.

The growth-rate distribution histogram in Figure 8 shows the coexistence of two different populations of crystals. The kinetic analysis indicates that the PCL crystallites are oriented predominantly with the crystallographic *b*-axis parallel to the plane of the PTFE surface. However, some PCL crystals are found to be oriented with the *a*-axis parallel to the substrate plane (situation B, Figure 7), implying that the $(010)_{\text{PCL}}$ plane is in contact with the PTFE substrate. An occurrence probability equal to 20% is estimated for such growth, based on the total number of crystal faces investigated of 47 (Figure 8). For this orientation a lattice matching (Δ) can be quantified via the following relation:

$$\Delta = \frac{2a_{\text{PCL}} - 3a_{\text{PTFE}}}{3a_{\text{PTFE}}} = 12\%$$

This lattice mismatch is about the same as the match previously determined for the $(100)_{\text{PCL}}\|(100)_{\text{PTFE}}$ interface. However, the representation of the $a-c$ PCL plane parallel to the closed-packed PTFE substrate in Figure 6B shows a molecular arrangement at the interface that is less favorable in terms of minimization of the adsorbate−substrate interaction energy, leading to an interface less often encountered.

Figure 9 shows a sequence of higher magnification images of a PTFE fibril obtained under isothermal crystallization conditions at the temperature of 56 °C. The PTFE chain direction is indicated by the added black arrows and can be used as an orientation marker. The images shown are amplitude images, as the phase response of the cantilever after PCL melting was mainly determined by the stiffness of the underlying PTFE substrate.

It can be clearly seen that the PCL crystals align with their basal facets perpendicular to the PTFE chain direction, which is in agreement with the crystal orientation determined in the previous section. The numerous crystals are observed to be distributed in two distinct populations, which differ in lamellar crystal widths. Compare, for example, the lamellae labeled J and K in the amplitude image of Figure 9A. All crystals can be seen protruding out from the PTFE substrate with similar heights. While initially mainly type-J crystals are observed at the PTFE surface, crystals of type K become more dominant later in time. Although the crystals have the same orientation, the precise reason for their different appearance remains unclear. Careful viewing reveals that the different types of crystals are seemingly randomly distributed on the PTFE substrate. Furthermore, the center of the crystals, i.e., the primary nuclei from which the crystal developed, cannot be related to the surface topography of grooves.

In addition to the major fraction of lamellar orientations parallel to the PTFE *c*-axis, a third population (type L) can be observed. The L-type crystals are identified by white dots placed on their center in the amplitude image of Figure 9. Such crystals are, however, relatively rare and are only observed later in time during the crystallization process. AFM imaging at higher magnification affords an even more detailed look at the points of origin. These images of the PTFE surface before and after growth of the type-L crystals are shown in parts A and B of Figure 10, respectively. The image in Figure 10B corresponds to an elapsed time of 16 h. It can be seen in the images that the crystals originate from steep valleys (grooves, black areas in the height image) on the PTFE surface. Some type of graphoepitaxial mechanism appears to cause the nucleation of these crystals. The spatial distribution of the crystals is in close relationship with the grating-like nature of the friction-deposited PTFE.

It is interesting to note that the type-L crystals are aligned parallel to the long directions of the grooves. As shown in the amplitude images of Figure 9B,C, these crystals grow along the two directions parallel to the substrate surface, and they increase in size along both parallel and perpendicular fibril directions, while J- and K-type crystals only show considerable growth in the perpendicular direction. Note that the growth of J- and

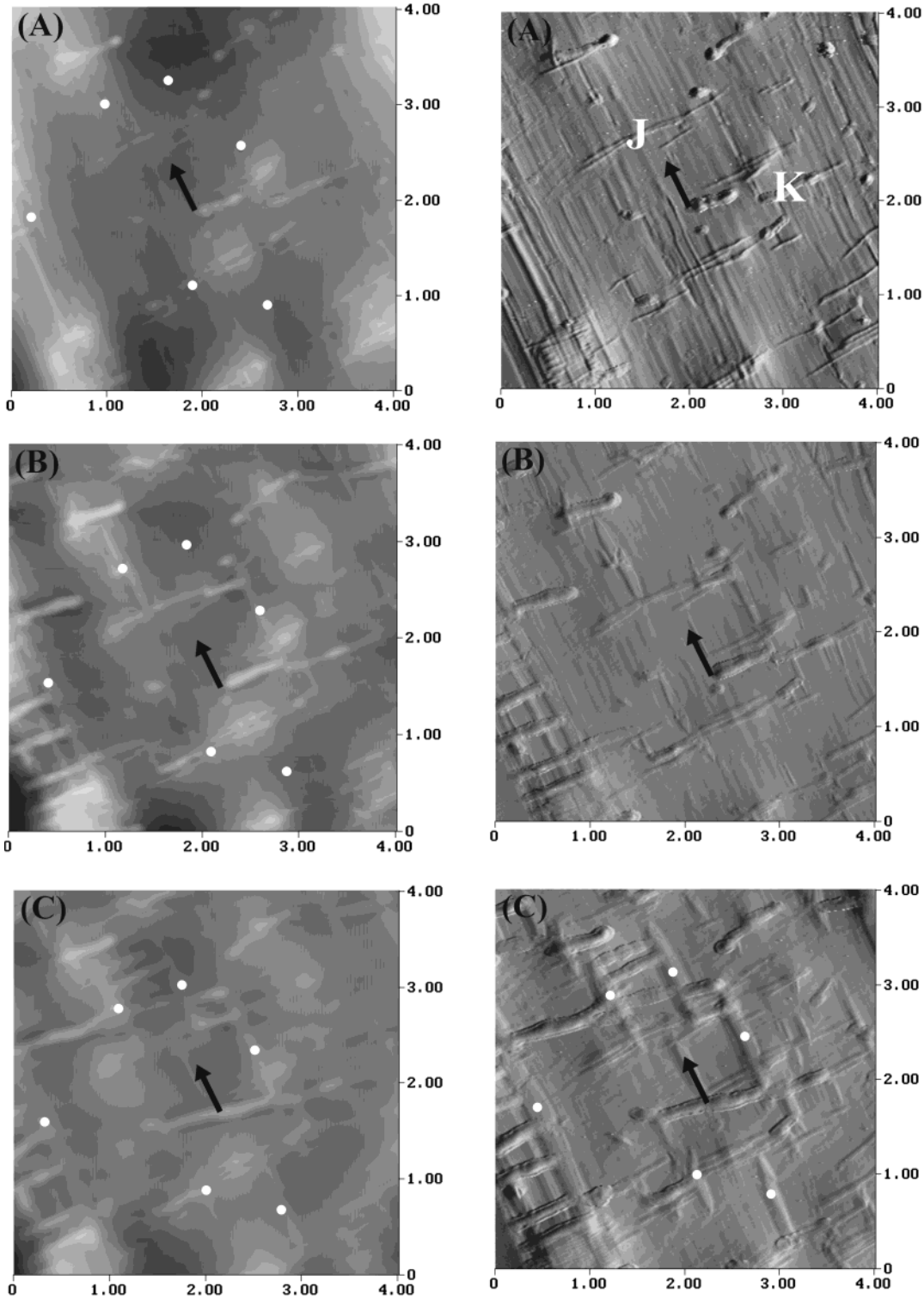

Figure 9. (A, C) AFM images of PCL crystal growth on a PTFE fibril at 56 °C. The left column displays height images, vertical scale is 200 nm (dark to bright), while the right column displays the corresponding amplitude images. The images in (B) and (C) correspond to elapsed time of 6 and 15 h, respectively, with respect to the image in (A). The black arrows indicate the orientation of the PTFE chains, and the center of the type-L crystals is identified by the white dots.

K-type crystals in the parallel direction was confined to an increase of several tens of nanometers, which suggests that the crystals are thickening during the isothermal crystallization.[26] The morphological habit of the type-L crystals indicates that the PCL chain's axis in these crystals is aligned perpendicularly to the PTFE surface. The view of the crystals therefore corresponds to a flat-on view. The crystal exhibits a lenticular shape with curved growth faces that extend toward the apex of the lamellae. The axial ratio indicates that the crystal growth rates are highly anisotropic. Note that the [010] direction has been identified as the fastest growth direction for PCL.[14] This indicates that the type-L crystals align with their *b*-axis parallel to the PTFE chain axis (Figure 10B). However, the nucleation process of the type-L crystals appears to have limited impact on the overall nucleation ability of PTFE toward PCL. The crystals possess a very high induction time

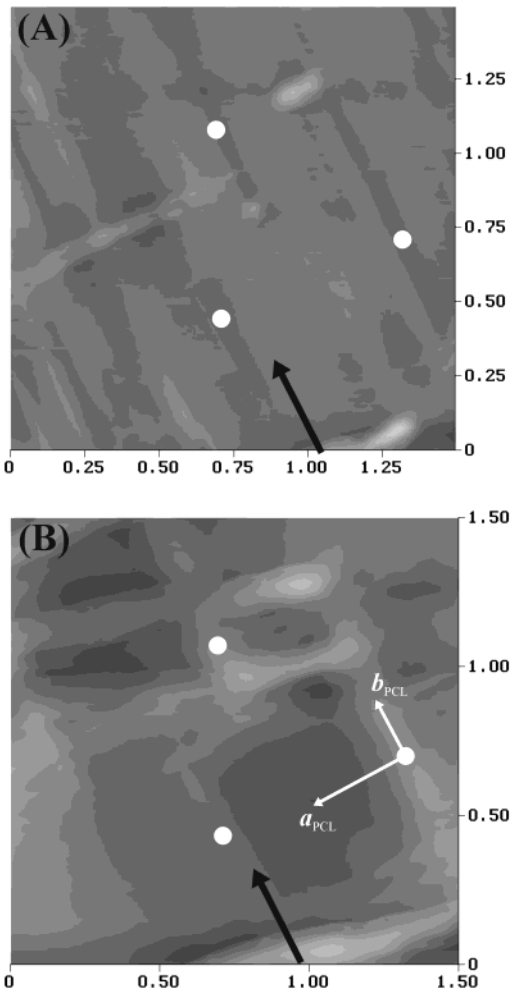

Figure 10. (A, B) AFM height images of PCL crystal growth on a PTFE fibril obtained at a temperature of 56 °C. The image in (B) corresponds to elapsed time of 16 h with respect to the image in (A). The vertical scale is 100 nm (dark to bright). The black arrows indicate the molecular orientation of the PTFE chains, and the center of the type-L crystals is identified by the white dots.

compared to the epitaxial nucleated crystals and are therefore not observed in the lower magnification images of Figure 4.

Conclusions

The study of the crystal growth of PCL on highly oriented PTFE fibrils prepared by the friction-transfer method has revealed specific features of the nucleation process. It is demonstrated that PTFE is an effective nucleating agent for PCL. In fact, three different orientations with different nucleation rates were observed. A lattice-matching between the *b*-axis of PCL (4.98 Å) and the corresponding interchain distance in the substrate crystal face appears to be the prominent feature relevant for epitaxy. In addition, the ordered (100) PTFE surface could also induce the growth of PCL crystals, with the a_{PCL} (7.48 Å) parallel to this plane. This latter epitaxy, however, was not preferred and only observed in a minor amount. Our study also showed the existence of a third population of crystals with a different orientation appearing later in time. These crystals were oriented with their b_{PCL} and a_{PCL} axes respectively parallel and perpendicular to the PTFE chain axis. The center of the crystal was closely related to the PTFE surface morphology, indicating the occurrence, to a certain extent, of the graphoepitaxy nucleation process.

This study also demonstrated the ability of AFM to image the nucleation process in real time on a lamellar scale on the foreign substrate. An understanding of the interactions at the substrate surface could be obtained by determination of lamellar-crystal orientation based on the analysis of the kinetic data.

Acknowledgment. L.G.M. Beekmans thanks the Dutch Foundation for Chemical Research (NWO−CW) for a graduate research fellowship. The authors are grateful to Prof. S. Muñoz-Guerra (Universitat Politècnica de Catalunya) for helpful discussions and revision of the manuscript.

References and Notes

(1) Binsbergen, F. L. In *Heterogeneous Nucleation of Crystallization*; McCaldin, M. J., Somorjai, G., Eds.; Pergamon: Oxford, 1973; Vol. 8, p 189.
(2) Wittmann, J. C.; Lotz, B. *Prog. Polym. Sci.* **1990**, *3150*, 909.
(3) Yan, S.; Katzenberg, F.; Petermann, J.; Yang, D.; Shen, Y.; Straupe, C.; Wittmann, J. C.; Lotz, B. *Polymer* **2000**, *41*, 2613.
(4) Yan, S.; Bonnet, M.; Petermann, J. *Polymer* **2000**, *41*, 1139.
(5) Yan, S.; Petermann, J.; Yang, D. C. *J. Polym. Sci., Polym. Phys.* **1997**, *35*, 1415.
(6) Wittmann, J. C.; Smith, P. *Nature (London)* **1991**, *352*, 414.
(7) Schönherr, H.; Vancso, G. J. *Polymer* **1998**, *39*, 5705.
(8) Yan, S.; Spath, T.; Petermann, J. *Polymer* **2000**, *41*, 4863.
(9) Fenwick, D.; Smith, P.; Wittmann, J. C. *J. Mater. Sci.* **1996**, *31*, 128.
(10) Vallee, R.; Damman, P.; Dosiere, M.; Toussaere, E.; Zyss, J. *J. Am. Chem. Soc.* **2000**, *122*, 6701.
(11) Hobbs, J. K.; McMaster, T. J.; Miles, M. J.; Barham, P. J. *Polymer* **1998**, *39*, 2437.
(12) Schultz, J. M.; Miles, M. J. *J. Polym. Sci., Polym. Phys.* **1998**, *36*, 2311.
(13) Pearce, R.; Vancso, G. J. *Macromolecules* **1997**, *30*, 5843.
(14) Beekmans, L. G. M.; Vancso, G. J. *Polymer* **2000**, *41*, 8975.
(15) Vancso, G. J.; Beekmans, L. G. M.; Pearce, R.; Trifonova, D.; Varga, J. *J. Macromol. Sci., Phys.* **1999**, *B38*, 491.
(16) Wittmann, J. C.; Hodge, A. M.; Lotz, B. *J. Polym. Sci., Polym. Phys.* **1983**, *21*, 2495.
(17) Kruger, J. K.; Prechtl, M.; Smith, P.; Meyer, S.; Wittmann, J. C. *J. Polym. Sci., Polym. Phys.* **1992**, *30*, 1173.
(18) Beekmans, L. G. M.; Vancso, G. J. *Probe Microsc.*, in press.
(19) Beekmans, L. G. M.; van der Meer, D. W.; Vancso, G. J. *Polymer* **2002**, *43*, 1887.
(20) Keith, H. D.; Padden, F. J., Jr. *Macromolecules* **1996**, *29*, 776.
(21) Yan, S.; Petermann, J. *J. Polym. Sci., Polym. Phys.* **2000**, *38*, 80.
(22) Petermann, J.; Xu, Y. *J. Mater. Sci.* **1991**, *26*, 1211.
(23) Hu, H. L.; Dorset, D. L. *Macromolecules* **1990**, *23*, 4604.
(24) Bunn, C. W.; Howells, E. R. *Nature (London)* **1954**, *174*, 549.
(25) Hobbs, J. K.; Miles, M. J. *Macromolecules* **2001**, *34*, 353.
(26) Phillips, P. J.; Rensch, G. J. *J. Polym. Sci., Polym. Phys.* **1989**, *27*, 155.

MA020237A